APPLICATION OF DIFFERENT TURBULENCE MODELS FOR IMPROVING CONSTRUCTION OF SMALL-SCALE BOILER FIRED BY SOLID FUEL

by

Nebojša G. MANIĆ*[*]*, Vladimir V. JOVANOVIĆ, Dragoslava D. STOJILJKOVIĆ, and Zagorka M. BRAT

Fuel and Combustion Laboratory, Faculty of Mechanical Engineering,
University of Belgrade, Belgrade, Serbia

Original scientific paper
https://doi.org/10.2298/TSCI160627017M

Due to the rapid progress in computer hardware and software, CFD became a powerful and effective tool for implementation turbulence modeling in defined combustion mathematical models in the complex boiler geometries. In this paper the commercial CFD package, ANSYS FLUENT was used to model fluid flow through the boiler, in order to define velocity field and predict pressure drop. Mathematical modeling was carried out with application of Standard, RNG, and Realizable k-ε turbulence model using the constants presented in literature. Three boilers geometry were examined with application of three different turbulence models with variants, which means consideration of 7 turbulence model arrangements in FLUENT. The obtained model results are presented and compared with data collected from experimental tests. All experimental tests were performed according to procedures defined in the standard SRPS EN 303-5 and obtained results are presented in this paper for all three examined geometries. This approach was used for improving construction of boiler fired by solid fuel with heat output up to 35 kW and for selection of the most convenient construction.

Key words: *CFD, turbulence model, construction, small scale boiler, solid fuel*

Introduction

Small scale boilers fired by solid fuel with heat output up to 50 kW are used for central heating in households and as energy source in small scale industry. Nowadays in Serbia this type of boilers is mainly outdated with low efficiency, high emissions of hazardous components (CO and particulate matter) and poor design [1]. Considering that about 35% of heat energy in Serbia is used in households, investigations in this field are very useful providing the necessary basis for improvement of this type of combustion appliances [2]. Boiler design improvement could allow higher energy efficiency by increasing the appliance coefficient of performance (COP) together with reduction of gaseous and particulate matter (PM) emissions. This is necessary according to valid Serbian legislation

[*] Corresponding author, e-mail: nmanic@mas.bg.ac.rs

which promotes use of renewable energy sources and improvement of energy efficiency as required by EU Directives for emissions from small-scale combustion appliances [3]. Also, this process should be constantly present in the future boiler development according to guidelines for down scaling the heat outputs for this type of appliances for heat production in households due to implementation of hybrid systems with solar energy for example [4].

Boiler design improvement is complex, time consuming and expensive process, because it needs experimental verification. Due to the fast development and improvement of computer hardware in recent years, CFD with numerical methods and mathematical techniques were easily involved in different engineering software for 3-D modeling of turbulence and fluid flows in complex geometries. Of course, this is not a trivial task. It requires appropriate sub-models for simulation of all of the constitutive processes of the combustion: flow and heat/mass transfer and their interactions [5-7].

As the turbulence is one of the key components defining combustion process in stoves and small-scale boilers, the commercial CFD packages are widely used for combustion modeling through defining reactive fluid flows together with the stoichiometry and chemical reactions [5, 8, 9]. First step in this complicated algorithm is defining velocity field in considered geometry taking into account turbulence intensity and mass continuity. Application of CFD methods on flow through the combustion appliances should provide the velocity field, pressure drops and "dead zones" in boiler geometry (zones where the velocity of flowing fluids are much slower than in the other). Those valuable data could save the time and money because they can trace the direction for design improvements without time consuming prototyping and testing but experiments are inevitable in order to get model verifications. If the experimental results approximately match the model results, CFD model is confirmed and it could be used for solving the similar problems. Turbulence modeling with different approaches could improve modeling process of fluid flow in boiler geometry [10, 11]. This is important in whole process of boiler design improvement and represents important factor in overall energy efficiency improvement of this type of combustion appliances.

The CFD modeling in this paper is related to fluid flow during the fixed bed combustion of small-scale solid fuel boiler with heat output of 35 kW. Applied approach involved only cold flow analysis, disregarding any combustion reactions in the whole combustion chamber.

Turbulence modeling

Turbulence modeling through the CFD commonly includes the use of two concepts, Eddy viscosity and Eddy diffusivity concept [9, 10, 12-15]. Bousinesq's hypothesis is the base of Eddy viscosity concept and it introduces assumption that Reynolds turbulent stress is proportional to velocity gradients. The Eddy diffusivity concept describes the process of heat and mass transfer at intense mixing which is characteristic of turbulent flow.

The Boussinesq's hypothesis is used in the Spalart-Allmaras model, the k-ε models, and the k-ω models. The advantage of this approach is the relatively low computational cost associated with the computation of the turbulent viscosity μ_t. In the case of the Spalart-Allmaras model, only one additional transport equation (representing turbulent viscosity) is solved. In the case of the k-ε and k-ω models, two additional transport equations (for the turbulence kinetic energy, k, and either the turbulence dissipation rate, ε, or the specific dissipation rate, ω) are solved, and μ_t is computed as a function of k and ε or k and ω. The disadvantage of the Boussinesq's hypothesis as presented is that it assumes μ_t is an isotropic scalar quantity, which is not strictly true.

The alternative approach, embodied in the Reynolds stress model (RSM), is to solve transport equations for each of the terms in the Reynolds stress tensor. An additional scale-determining equation (normally for ε) is also required. This means that five additional transport equations are required in 2-D flows and seven additional transport equations must be solved in 3-D.

In many cases, models based on the Boussinesq's hypothesis perform very well, and the additional computational expense of the Reynolds stress model is not justified. However, the RSM is clearly superior in situations where the anisotropy of turbulence has a dominant effect on the mean flow. Such cases include highly swirling flows and stress-driven secondary flows.

Mathematical formulation

Turbulence model have to be introduced in order to close the system of defined constitutive equations, and this model should be broadly applicable, accurate, easy and economical. One of the most commonly used turbulence model is the k-ε model which define equations for k (turbulence kinetic energy) together with ε (turbulent kinetic energy dissipation rate) and is developed into three forms.

(1) Standard k-ε turbulence model [9, 13-18]

Standard k-ε turbulence model was introduced for modeling of fully developed turbulent flows (corresponding to high Re numbers) where the value of molecular viscosity is neglected:

$$\frac{\mathrm{D}k}{\mathrm{D}t}=\nu_t\left(\frac{\partial U_i}{\partial x_j}+\frac{\partial U_j}{\partial x_i}\right)\frac{\partial U_i}{\partial x_j}-\varepsilon+\frac{\partial}{\partial x_j}\left[\left(\nu+\frac{\nu_t}{\sigma_k}\right)\frac{\partial k}{\partial x_j}\right] \tag{1}$$

However, by using appropriate near wall treatment standard k-ε turbulence model can be used for modeling of wide range of turbulent flows.

By multiplying the defined eq. (1) with ε/k and introducing the model coefficients, the final form of the equation for the turbulent kinetic energy dissipation rate ε is obtained. In its final form, the equation for ε consists of members who include production, dissipation, viscous diffusion and turbulent diffusion:

$$\frac{\mathrm{D}\varepsilon}{\mathrm{D}t}=C_{\varepsilon1}\frac{\varepsilon}{k}\nu_t\left(\frac{\partial U_i}{\partial x_j}+\frac{\partial U_j}{\partial x_i}\right)\frac{\partial U_i}{\partial x_j}-C_{\varepsilon2}f_2\frac{\varepsilon^2}{k}+E_\varepsilon+$$
$$+\frac{\partial}{\partial x_j}\left[\left(\nu+\frac{\nu_t}{\sigma_\varepsilon}\right)\frac{\partial\varepsilon}{\partial x_j}\right]+2\nu\nu_t\left(\frac{\partial^2 U_i}{\partial x_j^2}\right)^2 \tag{2}$$

where f_2 is a damping coefficient which, depending on applied turbulence model, that takes one of the following values:

– Jones and Lounder (abb. JL) [19]:

$$f_2 = 1 - 0.3\,\mathrm{e}^{-R_t^2} \tag{3}$$

– Chien (abb. C) [20]:

$$f_2 = 1 - 0.22\,\mathrm{e}^{\left(-\frac{R_t}{6}\right)^2} \tag{4}$$

– Launder – Sharma with Yap correction (abb. LSY) [21]:

$$f_2 = 1 - 0.3\,\mathrm{e}^{-R_t^2} \tag{5}$$

– Abe, Kondoh, and Nagano (abb. AKN) [22]:

$$f_2 = \left[1 - \mathrm{e}^{-(y^*/3.1)}\right]^2 \left[1 - 0.3\,\mathrm{e}^{-(R_t/6.5)^2}\right] \tag{6}$$

For the turbulent flow of viscous fluid, a turbulent viscosity term is introduced. Turbulent viscosity does not depend on fluid characteristics, but depends only on turbulence characteristics. In that case, effective viscosity is defined as a sum of molecular viscosity and turbulent viscosity of the fluid, as follows:

$$\mu = \mu_k + \mu_t \tag{7}$$

Turbulent kinematic viscosity is defined with the following formula:

$$\nu_\mathrm{t} = C_\mu \frac{k^2}{\varepsilon} \tag{8}$$

where C_μ is a coefficient whose value is defined in the field of turbulent boundary layer in which the Universal logarithmic wall law is applied and where all phenomena, except turbulence production and dissipation, can be neglected:

$$C_\mu = \left(u_*^2 / k\right)^2 \tag{9}$$

Considering equation for the turbulent kinetic energy dissipation rate ε, with adopting of the assumption about energy balance within the logarithmic part of turbulent boundary layer where the convective part can be neglected, and by introducing the appropriate relation, the form for determination of the coefficient $C_{\varepsilon 1}$ is:

$$C_{\varepsilon 1} = C_{\varepsilon 2} - \frac{\kappa^2}{\sqrt{C_\mu}\,\sigma_\varepsilon} \tag{10}$$

The coefficient $C_{\varepsilon 2}$ is defined for the zone with low velocity gradients, where the turbulence production and diffusion can be neglected, and where the dissipation of turbulent kinetic energy k can be determined as an exponential dependence $k \propto x^{-m}$. The formula for $C_{\varepsilon 2}$ coefficient determination is derived by adopting the mentioned assumptions and by introducing exponential dependence for k and ε:

$$C_{\varepsilon 2} = \frac{m+1}{m} \tag{11}$$

The remaining two constants σ_k and σ_ε are determined empirically, by applying the model in different cases of usual classical flows.

Table 1. Standard *k-ε* model constants

Model constant	JL	C	LSY	AKN
$C_{\varepsilon 1}$	1.55	1.35	1.44	1.50
$C_{\varepsilon 2}$	2.00	1.80	1.92	1.90
σ_k	1.00	1.00	1.00	1.40
σ_ε	1.30	1.30	1.30	1.40
C_μ	0.09	0.09	0.09	0.09

(2) Renormalization group k-ε turbulence model [9, 13-18]

Improvement of the standard model was made in order to increase accuracy and facilitate wider implementation of new turbulence models. RNG *k-ε* turbulence model is similar to the standard *k-ε* model, but it includes an additional member in the equation for *ε* which takes into consideration relation between turbulence dissipation and shear, acting of vorticity on turbulence, analytical formula for Prandtl number (standard model imply constant value of Prandtl number) and differential equation for effective viscosity. By using RNG *k-ε* turbulence model, two additional equations for turbulence kinetic energy and turbulent kinetic energy dissipation rate are introduced:

$$\frac{\mathrm{D}k}{\mathrm{D}t}=\frac{\partial}{\partial x_j}\left(\alpha_k \nu \frac{\partial k}{\partial x_j}\right)+\nu_\mathrm{t}\left(\frac{\partial U_i}{\partial x_j}+\frac{\partial U_j}{\partial x_i}\right)\frac{\partial U_i}{\partial x_j}-\varepsilon \tag{12}$$

$$\frac{\mathrm{D}\varepsilon}{\mathrm{D}t}=\frac{\partial}{\partial x_j}\left(\alpha_\varepsilon \nu \frac{\partial \varepsilon}{\partial x_j}\right)+C_{\varepsilon 1}\frac{\varepsilon}{k}P_k-C_{\varepsilon 2}^{*}\frac{\varepsilon^2}{k} \tag{13}$$

where α_k, α_ε – inverse values of the turbulent Prandtl number for k and ε.

Listed values are to be determined according to the following analytical formula:

$$\left|\frac{\alpha-1.3929}{\alpha_0-1.3929}\right|^{0.6321}\left|\frac{\alpha+2.3929}{\alpha_0+2.3929}\right|^{0.3679}=\frac{\mu_k}{\mu} \tag{14}$$

For fully developed turbulent flow in the area of high Reynolds numbers follows:

$$\frac{\mu_k}{\mu}\ll 1,\ \ \alpha_k=\alpha_\varepsilon\cong 1.393 \tag{15}$$

Table 2. RNG *k-ε* model constants

$C_{\varepsilon 1}$	$C_{\varepsilon 2}$	C_μ
1.42	1.68	0.0845

The RNG *k-ε* turbulence model in this paper was considered in 2 variants depends of excluding (RNGv1) or including (RNGv2) differential viscosity model [23]. This viscosity model specifies whether or not the low-Reynolds-number RNG modifications to turbulent viscosity should be included.

(3) Realizable k-ε turbulence model [9, 13-18]

Realizable k-ε turbulence model eq. (16), for turbulence kinetic energy takes from the standard k-ε turbulence model, while eq. (17) for the rate of dissipation of the turbulence kinetic energy is additionally improved with variable constant C_μ so the normal stress value in the Boussinesq's hypothesis can be feasible. Further improvement of the model is accomplished by introduction of the new equation for the turbulent kinetic energy dissipation rate which takes into consideration vortices fluctuations:

$$\frac{\mathrm{D}k}{\mathrm{D}t}=\frac{\partial}{\partial x_j}\left[\left(\nu+\frac{\nu_\mathrm{t}}{\sigma_k}\right)\frac{\partial k}{\partial x_j}\right]+\nu_\mathrm{t}\left(\frac{\partial U_i}{\partial x_j}+\frac{\partial U_j}{\partial x_i}\right)\frac{\partial U_i}{\partial x_j}-\varepsilon \tag{16}$$

$$\frac{\mathrm{D}\varepsilon}{\mathrm{D}t}=\frac{\partial}{\partial x_j}\left[\left(\nu+\frac{\nu_\mathrm{t}}{\sigma_\varepsilon}\right)\frac{\partial \varepsilon}{\partial x_j}\right]-C_2\frac{\varepsilon^2}{k+\sqrt{\nu\varepsilon}} \tag{17}$$

Table 3. Realizable *k-ε* model constants

C_2	σ_k	σ_ε
1.9	1.0	1.2

The CFD approach, geometry and mesh

Mathematical modeling of fluid flow in the boiler geometry was carried out with commercial CFD package ANSYS Fluent including the viscous model according to different arrangement of turbulence models. Boundary surfaces on considered boiler geometries for each case separately are presented on fig. 1 and used to set boundary conditions as air inlet (AIR_in) defined as mass flow inlet in ANSYS Fluent and flue gas outlet (FG_out) defined as pressure outlet. All other surfaces presented on analyzed boiler geometries represent wall surface at considered domen and define as stationary wall (WALL) boundary condition in Fluent. Values of mass flow at boundary air inlet are defined and calculated according to experimental results for considered geometry and used fuel and will be presented in the section Experimental tests and results (tab. 7).

Three different boiler geometries were analyzed which differ by position of combustion air entrance, boiler grate position and the arrangement of flue gas removal. Position of the combustion air entrance and the boiler grate, measured from the bottom of the appliance, as well as flue gas removal arrangement for all considered geometries are given in tab. 4 and the analyzed geometries are presented in fig. 1.

Table 4. Data for different geometries

	Boiler grate position* [mm]	Combustion air entrance position	Flue gas removal arrangement
Case 1	65	Above the grate	Vertical from above
Case 2	145	In line with the grate	Horizontal from backside
Case 3	145	Below the grate	Horizontal from backside

*measured from the bottom

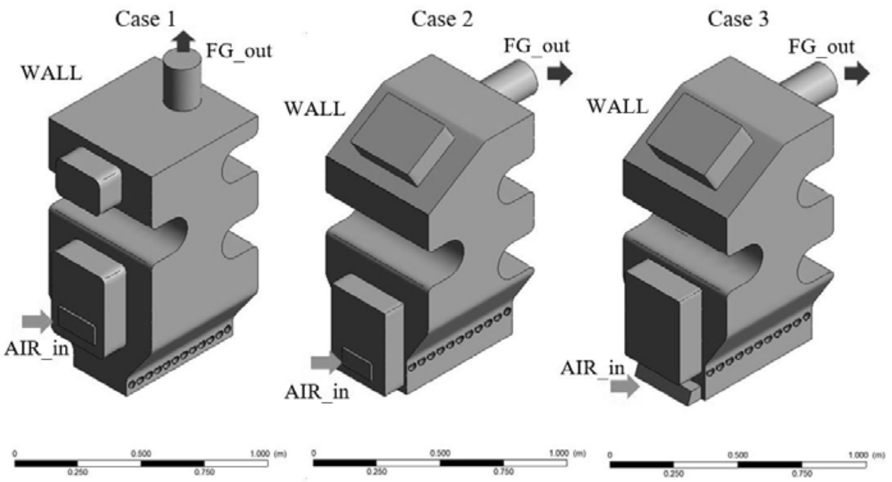

Figure 1. Analyzed boiler geometries *(for color image see journal website)*

In order to apply CFD to considered cases, the tetrahedral mesh was generated for all three boiler geometries and number of nodes for each mesh grid is given in tab. 5.

Table 5. Mesh data

–	Case 1	Case 2	Case 3
Number of nodes	55470	66307	50158

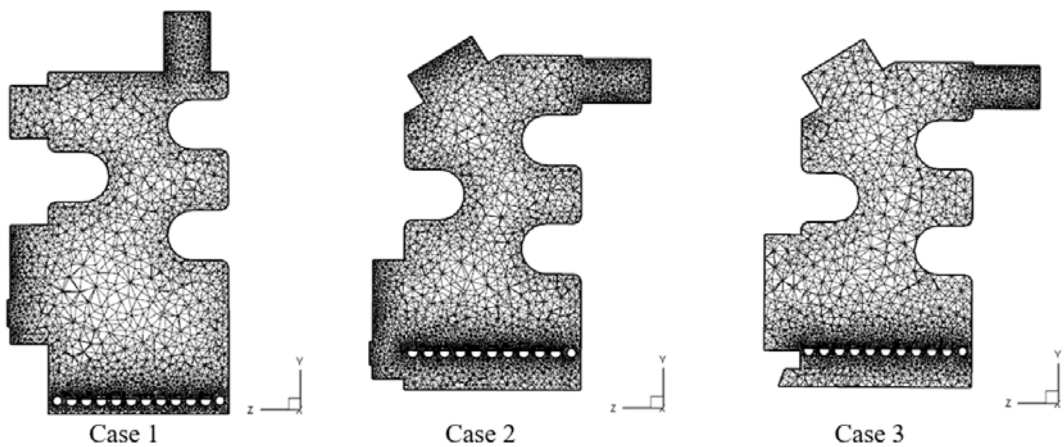

Figure 2. Cross-section of generated meshes for analyzed cases

According to high number of analyzed variants in order to optimize computational process number of nodes was chosen and generation of mesh was carried out and in order to fulfill mesh orthogonal quality required by CFD software [23]. However numerical solution must be grid independent but the grid independence study was too complex for the scope of this paper regarding many (twenty one) analyzed cases. Cross-sections of generated meshes for all three analyzed cases in YZ plane at x = 285 mm from the side wall of the boiler are presented on fig. 2.

Discretization of the results in CFD package was made by SIMPLE scheme for pressure-velocity coupling and second order upwind for pressure and momentum together with first order upwind for turbulent kinetic energy and turbulent dissipation rate spatial discretization. Solution methods were carried out with ANSYS FLUENT default convergence criteria, solution controls and residuals monitors [24].

Experimental tests and results

Household hot water boiler fired by solid fuel with declared thermal output of 35 kW was used for all experimental tests in this paper. Three different boiler geometries were examined differed by position of combustion air entrance, boiler grate position and the arrangement of flue gas removal as given in tab. 4 and presented in fig. 1.

Analyzed boiler geometries were tested on the test installation designed and constructed in Fuel and Combustion Laboratory at the Faculty of Mechanical Engineering, as defined in SRPS EN 303-5 (fig. 4). Test installation consists of tested appliance, weighing scale and measurement sections for flue gas analysis, flue gas and ambient air pressure and temperature and water flow rate together with data acquisition system for collecting all measurement data.

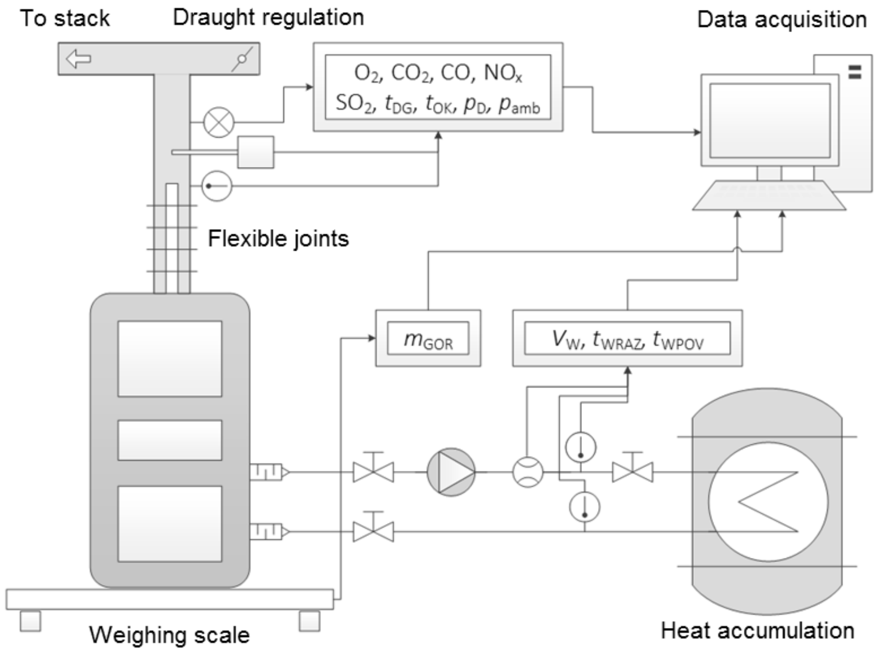

Figure 3. Test installation *(for color image see journal website)*

All experimental tests were carried out according to the procedure defined in SRPS EN 303-5 and only partial tests were made for determining measurement data and calculation of values which should exhibit energy efficiency boiler construction improvement. For all experimental tests beech wood was used as test fuel, prepared according to standard demands.

Proximate and ultimate analysis of test fuel was made according to the standard SRPS EN ISO 17225 and results (for as received mass) are given in tab. 6.

Table 6. Proximate and ultimate analysis of test fuel

PROXIMATE ANALYSIS	
Total moisture (% m/m)	21.35
Ash (% m/m)	0.81
Combustibles (% m/m)	77.84
Volatiles (% m/m)	66.77
Low heating value (kJ/kg)	13930
ULTIMATE ANALYSIS	
Carbon (% m/m)	33.17
Hydrogen (% m/m)	4.74
Nitrogen (% m/m)	0.17
Sulphur (% m/m)	0.00
Oxygen, as difference (% m/m)	39.75

Average values of measurement data together with calculated values (according to the standard) important for presenting improvement of boiler construction energy efficiency and measured pressure drops at flue gas damper for all analyzed boiler geometries (Case 1 to 3) are given in tab. 7.

Table 7. Experimental test results for examined boiler geometries

SRPS EN 303-5 (Partial test)	Unit	Case 1	Case 2	Case 3
m_{GOR}	kg/h	8.8	7.9	9.7
O_2	%	15.98	11.52	10.72
CO_2	%	4.85	6.64	7.42
CO	ppm	1526	1443	1390
NO_x	ppm	71	133	122
t_{DG}	°C	270.8	273.0	252.8
t_{WRAZ}	°C	72.2	66.1	65.2
t_{WPOV}	°C	60.2	57.0	53.3
V_W	m3/h	1.54	1.90	2.10
$m_{VAZ} \cdot 10^2$	kg/s	3.56	1.69	1.91
Exp_PD	Pa	12	14	10
Heat input	kW	34.26	30.57	37.53
Heat output (direct method)	kW	21.40	20.31	29.00
Efficiency	%	62.46	66.44	77.29
CO emission at 10% O_2	mg/m^3	3040	2092	1859
NO_x emission at 10% O_2	mg/m^3	319	316	268
Excess air	--	4.18	2.21	2.04

Model results and discussion

Pressure drop (PD) in the considered geometries was calculated according to the mathematical model results as difference of average total pressures at boundary surfaces for fluid flow through the boiler defined as air inlet (AIR_in) and flue gas outlet (FG_Out). These calculations were carried out for 3 geometries and for 7 turbulence model arrangements and compared with experimental results (Exp_PD) which were measured for each case separately and shown in tab. 7.

Results of the average total pressures at boundary surfaces and calculated pressure drop as well as turbulence intensity (TI) in boiler volume according to the mathematical model results for case 1, 2 and 3 are given in tabs. 8, 9 and 10, respectively.

Table 8. Mathematical model results for Case 1

		JL	C	LSY	AKN	RNG v1	RNG v2	Realizable
TI	%	4.08	3.91	4.07	3.76	3.50	1.93	6.59
FG_Out	Pa	7.2	7.1	6.9	6.9	7.5	7.4	6.8
AIR_In	Pa	18.1	19.4	13.1	16.3	12.7	12.2	15.0
PD	Pa	10.9	12.3	6.2	9.4	5.2	4.8	8.2

Table 9. Mathematical model results for Case 2

		JL	C	LSY	AKN	RNG v1	RNG v2	Realizable
TI	%	4.74	3.78	3.79	3.79	3.52	2.20	4.67
FG_Out	Pa	7.2	6.8	7.0	6.9	7.1	6.4	6.9
AIR_In	Pa	24.6	20.6	23.2	23.1	16.8	29.3	21.1
PD	Pa	17.4	13.8	16.2	16.2	9.7	22.9	14.2

Table 10. Mathematical model results for Case 3

		JL	C	LSY	AKN	RNG v1	RNG v2	Realizable
TI	%	4.49	4.28	4.47	4.28	3.91	2.64	5.14
FG_Out	Pa	7.5	7.4	7.4	7.4	7.6	7.6	6.6
AIR_In	Pa	16.8	14.8	14.9	14.3	15.0	16.4	16.1
PD	Pa	9.3	7.4	7.5	6.9	7.4	8.8	9.5

In order to present CFD results of velocity field and turbulent intensity for each considered case, two different model results with the turbulence model arrangement that produced the best and the worst matching with experimental results of pressure drop were chosen.

According to boiler geometry dimensions (same width for each considered case) CFD results were presented in YZ plane at x = 285 mm from the side wall of the boiler. Velocity field and turbulent intensity for different cases for chosen turbulence model arrangement were presented as well:

– fig. 4, Case 1 according to C and RNG ver2 turbulent model arrangement,
– fig. 5, Case 2 according to Realizable and RNG ver2 turbulent model arrangement, and
– fig. 6, Case 3 according to Realizable and AKN turbulent model arrangement.

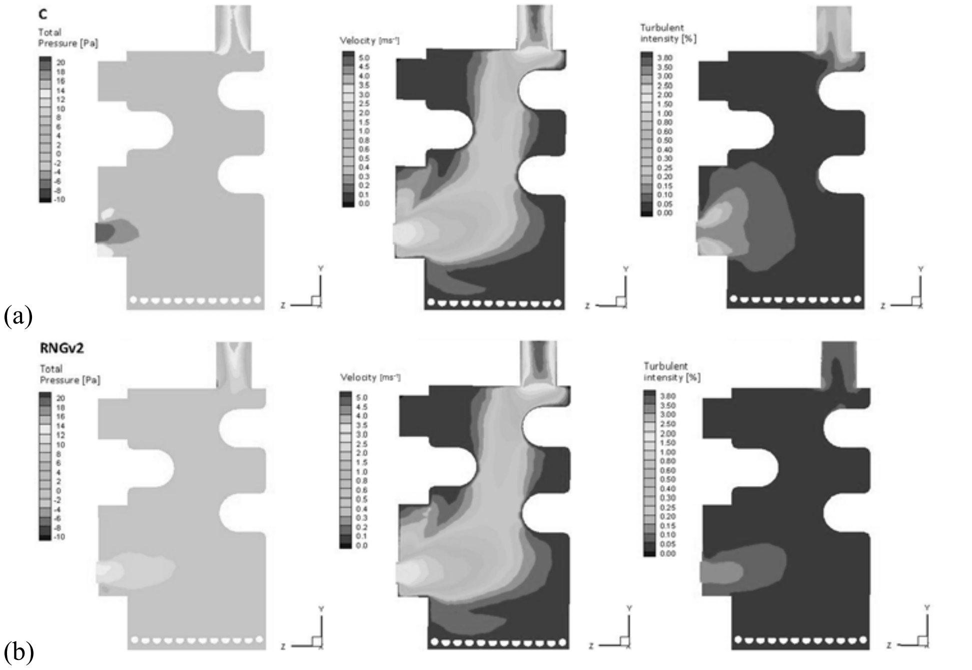

Figure 4. The best (a) and the worst (b) agreement of CFD and experimental results for Case 1
(for color image see journal website)

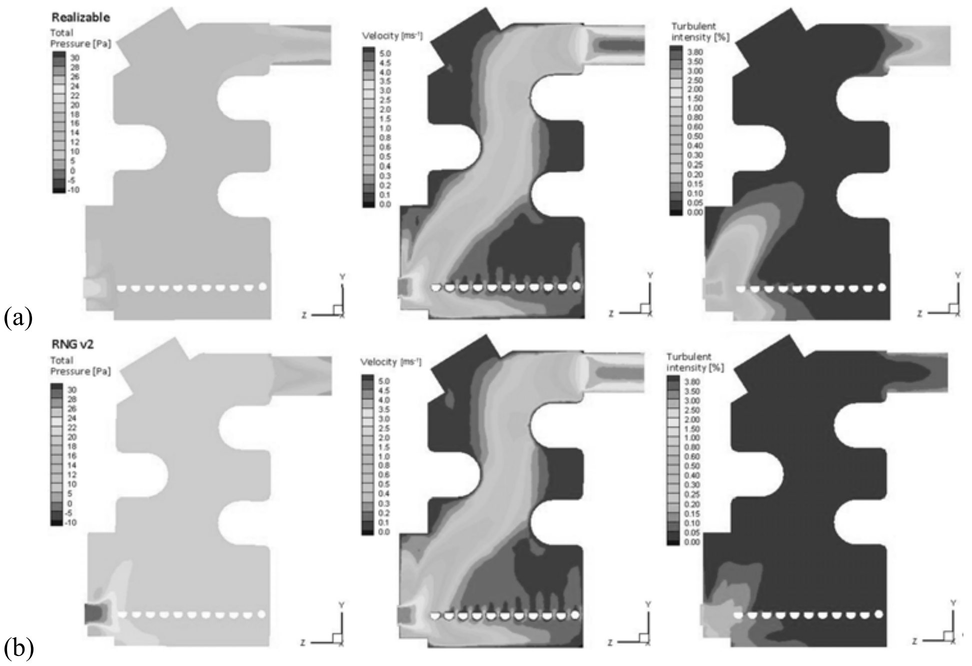

Figure 5. The best (a) and the worst (b) agreement of CFD and experimental results for Case 2
(for color image see journal website)

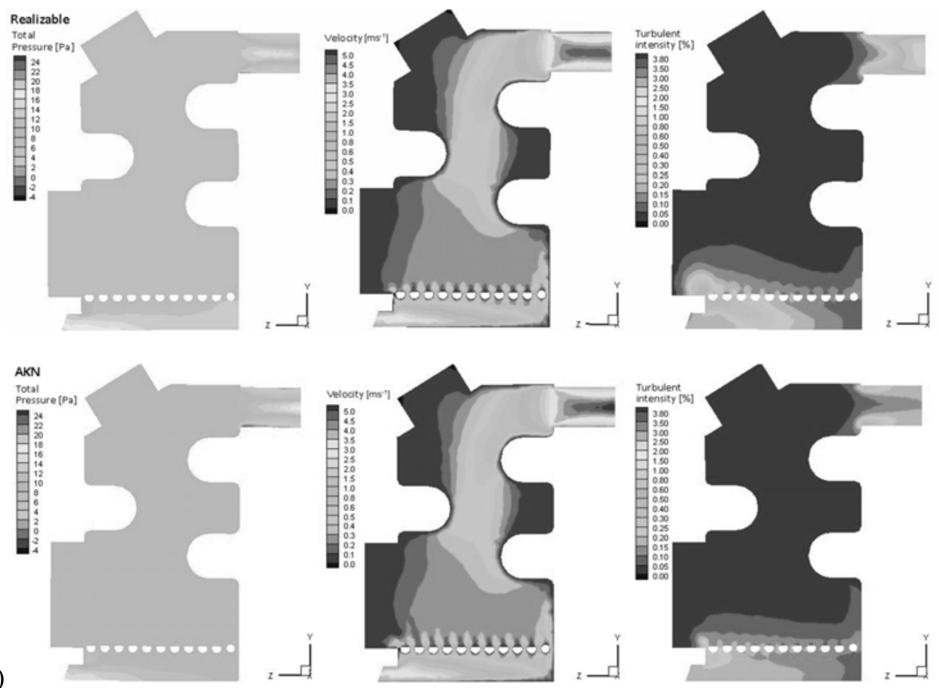

(a)

(b)

Figure 6. The best (a) and the worst (b) agreement of CFD and experimental results for Case 3
(for color image see journal website)

Analysis of model results presented on above figures indicates that turbulence model arrangements which achieve the best agreement for pressure drop through the boiler geometry with the experimental results also gives the higher turbulence intensity in the whole volume of the boiler combustion chamber. This is also noticed comparing values of turbulence intensity in the tabs. 8, 9, and 10 and is clearly indicated on figs. 4, 5, and 6 where turbulent intensity profiles are presented for the best (a) and worst (b) agreement for each analyzed boiler geometry.

Velocity fields in these two parts (a and b) of figures for each individual case are comparable and don't indicate the difference in intensity of turbulence. As mentioned before, turbulence intensity is one of the key parts for modeling combustion process and therefore one of the ultimate input parameters to be adopted before combustion model procedures for particular boiler geometry. This adoption could increase the combustion model precision and decrease the difference between model results and experimental data which could be used for model validation.

Different turbulent model arrangement for each case *i. e.* for each examined boiler geometry could have remarkable impact on total pressure, pressure drop and turbulent intensity thus significant impact on combustion process modeling in the boiler. Velocity fields for all turbulence arrangements are comparable for each three analyzed geometries and don't represent good combustion model indicators, but still can be used for selection of the most convenient geometry for air distribution and assessment of the fluid flow "dead zones" in the boiler volume. Choosing the best turbulent model approach for considered geometry is crucial for better definition of the model parameters which can be used in the next step of boiler construction improvement.

Conclusions

According to presented results of experimental tests and CFD analysis for three different boiler geometries with 7 turbulent model arrangements it can be concluded:

- Relatively low efficiency (between 62% up to 77%) and high CO emission (between 1859 mg/m^3 up to 3040 mg/m^3) of analyzed boiler geometries according to experimental tests shows the necessity for boiler construction improvement. Average values of experimental test results were adopted as model parameters for numerical analysis, and used as values for quantities at boundary conditions.
- For considered cases *i. e.* analyzed boiler geometries presented in this paper the C turbulent model arrangement provide the best agreement with the experimental results for pressure drop in Case 1 for boiler geometry with air inlet above the grate and vertical flue gas removal from the top of the boiler.
- The Realizable turbulent model arrangement provides the best match with the experimental results for pressure drop in Case 2 and Case 3 of boiler geometry with air inlet in line and below the grate and horizontal flue gas removal from the backside of the boiler.

According to analysis of CFD results (velocity field and turbulent intensity) in the selected cross section of the 3 considered boiler geometries it could be concluded that Case 3 of boiler geometry has the best fluid flow profile in the boiler. Analysis for boiler volume on fig. 5a shows the best air distribution over the grate and indicates the better combustion performance unlike the two other cases (figs. 3a and 4a). This conclusion could be also confirmed according to experimental results presented in tab. 7. Analyzing these results, the highest efficiency and the lowest emission values of all three analyzed geometries were obtained during the test of Case 3. Good air distribution is necessary for the complete combustion and for increase of the energy output (efficiency and heat output) together with decrease of the gaseous and PM emissions. Besides, with good air distribution fluid flow "dead zones" in the combustion chamber can be avoided or minimized which enables reduction of boiler dimensions and decrease of the production costs. Based on these conclusions, Case 3 of analyzed boiler geometry was selected as a template geometry for improvement of the construction of the analyzed combustion appliance and for further combustion modeling. Additionally, grid independency should be also taken into account for choosing the best numerical solution and this could be the explanation for the fact that different turbulent model arrangement provides the best matching with experimental data for Cases 2 and 3 unlike Case 1. In general, the results of mathematical models (especially if were obtained without experimental validation) are tightly connected with quality of grid for considered geometry, in order to use presented model for other boiler geometry improvement, increasing the grid quality together with the grid independency study will be the future work of the authors.

Nomenclature

A – model constant
C_μ – turbulence model coefficient
$C_{\varepsilon 1}$ – turbulence model coefficient
α_ε – inverse value for turbulent Prandtl number for
Γ – turbulent diffusion of heat or mass, [m^{2}s^{-1}]
ε – rate of dissipation of the turb. kin. energy, [m^{2}s^{-3}]

$C_{\varepsilon 2}$ – turbulence model coefficient
$D_{i,m}$ – oxidizer diffusion coefficient, [mm^2s^{-1}]
d_p – coke residue current diameter, [mm]
E – turbulence model term
$I_{\vec{u}}$ – turbulence intensity
k – turbulent kinetic energy, [m^2s^{-2}]
p – pressure, [Pa]
R_t – turbulent Reynolds number
t – temperature, [°C]
$\vec{u}$ – velocity, [ms^{-1}]
$\overline{u}$ – average velocity in x-direction, [ms^{-1}]
$\overline{v}$ – average velocity in y-direction, [ms^{-1}]
$\overline{w}$ – average velocity in z-direction, [ms^{-1}]
u' – velocity fluctuation in x-direction, [ms^{-1}]
v' – velocity fluctuation in y-direction, [ms^{-1}]
w' – velocity fluctuation in z-direction, [ms^{-1}]

Greek symbols

α_k – inverse value for turbulent Prandtl number for k
μ – effective dynamic viscosity, [Pa·s]
μ_t – turbulent dynamic viscosity, [Pa·s]
μ_k – molecular dynamic viscosity, [Pa·s]
ν – effective kinematic viscosity, [m^2s^{-1}]
ν_t – turbulent kinematic viscosity, [m^2s^{-1}]
ρ – density, [kgm^{-3}]
σ – turbulence model coefficient
σ_t – turbulent Prandtl number
τ – time, [s]
ϕ – free variable

Superscipts

* – normalized value
′ – fluctuation

Subscripts

k – quantity in k equation
t – turbulent quantity

References

[1] Glavonjic, B., *et al.*, Wood Pellets Market in Serbia – Production and Opportunities for Utilization, *Proceedings*, 19th European Biomass Conference & Exhibition, ETA-Florence Renewable Energies, Berlin, 2011, pp. 2543-2548
[2] Karakosta, C., *et al.*, Review and Analysis of Renewable Energy Perspectives in Serbia, *International Journal of Energy and Environment*, *2* (2011), 1, pp. 71-84
[3] ***, R.O. SERBIA, National Renewable Energy Action Plan of the Republic of Serbia, in: D.a.E.P. Ministry of Energy (Ed.) Belgrade, 2013, pp. 158
[4] Fiedler, F., Persson, T., Carbon Monoxide Emissions of Combined Pellet and Solar Heating Systems, *Applied Energy*, *86* (2009), 2, pp. 135-143
[5] Chaney, J., *et al.*, An Overview of CFD Modeling of Small-Scale Fixed-Bed Biomass Pellet Boilers with Preliminary Results from a Simplified Approach, *Energ Convers Manage*, *63* (2012), Nov., pp. 149-156
[6] Porteiro, J., *et al.*, Numerical Modeling of a Biomass Pellet Domestic Boiler, *Energy & Fuels*, *23* (2009), 2, pp. 1067-1075
[7] Klason, T., Bai, X.S., Computational Study of the Combustion Process and NO Formation in a Small-Scale Wood Pellet Furnace, *Fuel*, *86* (2007), July-Aug., pp.1465-1474
[8] Manic, N., Optimisation and Modeling of Combustion Process in Household Pellet Stoves (in Serbian), Ph. D. thesis, Faculty of Mechanical Engineering, University of Belgrade, Belgrade, 2011
[9] Amini, B., Khaleghi, H., A Comparative Study of Variant Turbulence Modeling in the Physical Behaviors of Diesel Spray Combustion, *Thermal Science*, *15* (2011), 4, pp. 1081-1093
[10] Sodja, J., Turbulence models in CFD, Ph. D. thesis, University of Ljubljana, Ljubljana, 2007
[11] Schnell, U., Numerical Modeling of Solid Fuel Combustion Processes Using Advanced CFD-Based Simulation Tools, *Progress in Computational Fluid Dynamics*, *1* (2001), 4, pp.208-218
[12] Davidson, L., An Introduction to Turbulence Models, Publication 97/2, Department of Thermo and Fluid Dynamics, Chalmers University of Technology, Gothenburg, Sweden, 2003
[13] Davidson, P. A., Turbulence: An Introduction for Scientists and Engineers, 2nd ed., Oxford University Press, New York, USA, 2015

[14] Wilcox, D. C., Turbulence Modeling for CFD, DCW industries La Canada, Cal., USA, 1998
[15] Bredberg, J., On Two Equation Eddy-Viscosity Models, Internal Report 01/8, Department of Thermo and Fluid Dynamics, Chalmers University of Technology, Gothenburg, Sweden, 2001
[16] Kolmogorov, A. N., The Local Structure of Turbulence in an Incompressible Fluid for Very Large Reynolds' Numbers, *Dokl. Akad. Nauk SSSR*, *30* (4), 1941, pp. 301-305
[17] Monin, A. S., Equations of Turbulent Motion, *Journal of Applied Mathematics and Mechanics*, *31* (1967), 6, pp. 1057-1068
[18] Harlow, F. H., Nakayama, P.I., Transport of Turbulence Energy Decay Rate, Report LA-3854, Los Alamos Scientific Lab., N. Mex., USA, 1968
[19] Lopez de Bertodano, M., *et al.*, Development of a k-ε Model for Bubbly Two-Phase Flow, *Journal of Fluids Engineering*, *116* (1994), 1, pp. 128-134
[20] Chien, K.-Y., Predictions of Channel and Boundary-Layer Flows with a Low-Reynolds-Number Turbulence Model, *AIAA Journal*, *20* (1982), 1, pp. 33-38
[21] Launder, B. E., Spalding, D. B., The Numerical Computation of Turbulent Flows, *Computer Methods in Applied Mechanics and Engineering*, *3* (1974), 2, pp. 269-289
[22] Abe, K., A New Turbulence Model for Predicting Fluid Flow and Heat Transfer in Separating and Reattaching Flows—I. Flow Field Calculations, *International Journal of Heat and Mass Transfer*, *37* (1994), 1, pp. 139-151
[23] ***, ANSYS Fluent 12.1 – User's Guide, in: F. Inc (Ed.) Lebanon, 2006.
[24] Lee, Y.-W., Assessment of Wood Pellet Combustion in a Domestic Stove, *Journal of Material Cycles and Waste Management*, *13 (3)* (2011), Sept., pp. 165-172

Paper submitted: June 27, 2016
Paper revised: July 29, 2016
Paper accepted: December 19, 2016